Hindawi
Journal of Spectroscopy
Volume 2017, Article ID 3565462, 5 pages
https://doi.org/10.1155/2017/3565462

Research Article

Optical Properties of Er^{3+}-Doped $CdIn_2O_4$ and $CdIn_2O_4$ Crystals

Tae Hwan Bang, Jong Wuk Kang, and Jin Jeong

Department of Physics, Chosun University, 309 Pilmun-daero, Dong-gu, Gwangju 501-759, Republic of Korea

Correspondence should be addressed to Jin Jeong; jeji@chosun.ac.kr

Received 29 August 2017; Accepted 7 November 2017; Published 25 December 2017

Academic Editor: Jau-Wern Chiou

$CdIn_2O_4$ and $CdIn_2O_4$:Er^{3+} crystals were grown by solid-state sintering of CdO and In_2O_3 with $ErCl_3$. X-ray diffraction analysis revealed that $CdIn_2O_4$ and $CdIn_2O_4$:Er^{3+} adopt a cubic structure with respective lattice constants of $a = 9.1655$ Å and $a = 9.1662$ Å. The optical absorption spectra obtained near the fundamental absorption edge showed that these compounds have a direct energy band gap. The photoluminescence (PL) spectra of $CdIn_2O_4$:Er^{3+} acquired in the wavelength range of 630–700 nm at 294 K showed peaks in the region of 651–686 nm and eight sharp emission peaks due to the Er^{3+} ions. These PL peaks were attributed to radiative transitions between the split electron energy levels of the Er^{3+} ions occupying the In^{3+} sites of the $CdIn_2O_4$ host lattice.

1. Introduction

$CdIn_2O_4$, a ternary semiconductor with the A-B-X composition, is an n-type semiconductor with a cubic structure that crystallizes in the Fd3m space group. $CdIn_2O_4$ has a wide optical energy gap and has been studied because of its high electrical conductivity and transparency in the visible light region. $CdIn_2O_4$ materials are applied in gas sensors and devices such as solar cells, flat panel displays, invisible security circuits, and windshield defrosters [1–5]. The energy gap, crystal structure, and photoluminescence (PL) of pure $CdIn_2O_4$ have been studied [4–6], but no research has been conducted on pure $CdIn_2O_4$ doped with 4f species. As a method of changing the electrical resistance of compound semiconductors and to widen the light energy region with photoelectric sensitivity, the effects of doping with 4f materials on the electrochemical characteristics should be evaluated. Although basic phenomena such as the characterized, photocatalytic activity, and evaluated photoelectrochemical water splitting for $CdIn_2O_4$ crystals [7, 8] doped with C and N, the energy gap and the photoluminescence spectrum of $CdIn_2O_4$:Er^{3+} have not been documented. In this study, the energy gap, photoluminescence spectrum, and crystal growth of $CdIn_2O_4$ and $CdIn_2O_4$:Er^{3+} materials crystallized at temperatures of 900, 1000, and 1050°C are investigated.

2. Materials and Methods

Growth of the $CdIn_2O_4$ and $CdIn_2O_4$:Er^{3+} crystalline crystals was achieved by employing high-purity (5 N) CdO and In_2O_3 powder; a mixture of these compounds based on weight was magnetically stirred for 2 h, and high-purity ethanol was added at a molar ratio of 1 : 1. To homogenize the mixed powder, the mixture was placed into a ball jar, mixed well with a mixer mill (Retsch, 200, Germany) and placed in an alumina crucible with a lid and the crucible which was then placed in a graphite crucible and filled with activated carbon. The graphite crucible was placed in the center of a low-temperature muffle furnace (Thermolyne, F48010-26, USA), and the temperature was first increased from room temperature to 800°C at a heating rate of 5°C/min, followed by sintering for 12 hours. The sintered powder sample was ground in an alumina crucible and powdered to achieve even mixing. The powder was mixed again in a mixer mill for about approximately 5 hours. The graphite crucible was then placed in the center of the furnace, where the temperature of the furnace (Thermolyne, F46120CM-33, USA), equipped with automatic thermostat could be controlled within the tolerance of 1°C at room temperature. The graphite crucible was then placed in the center of the furnace at 900~1050°C. The temperature was raised at a rate of 2°C/min and was maintained

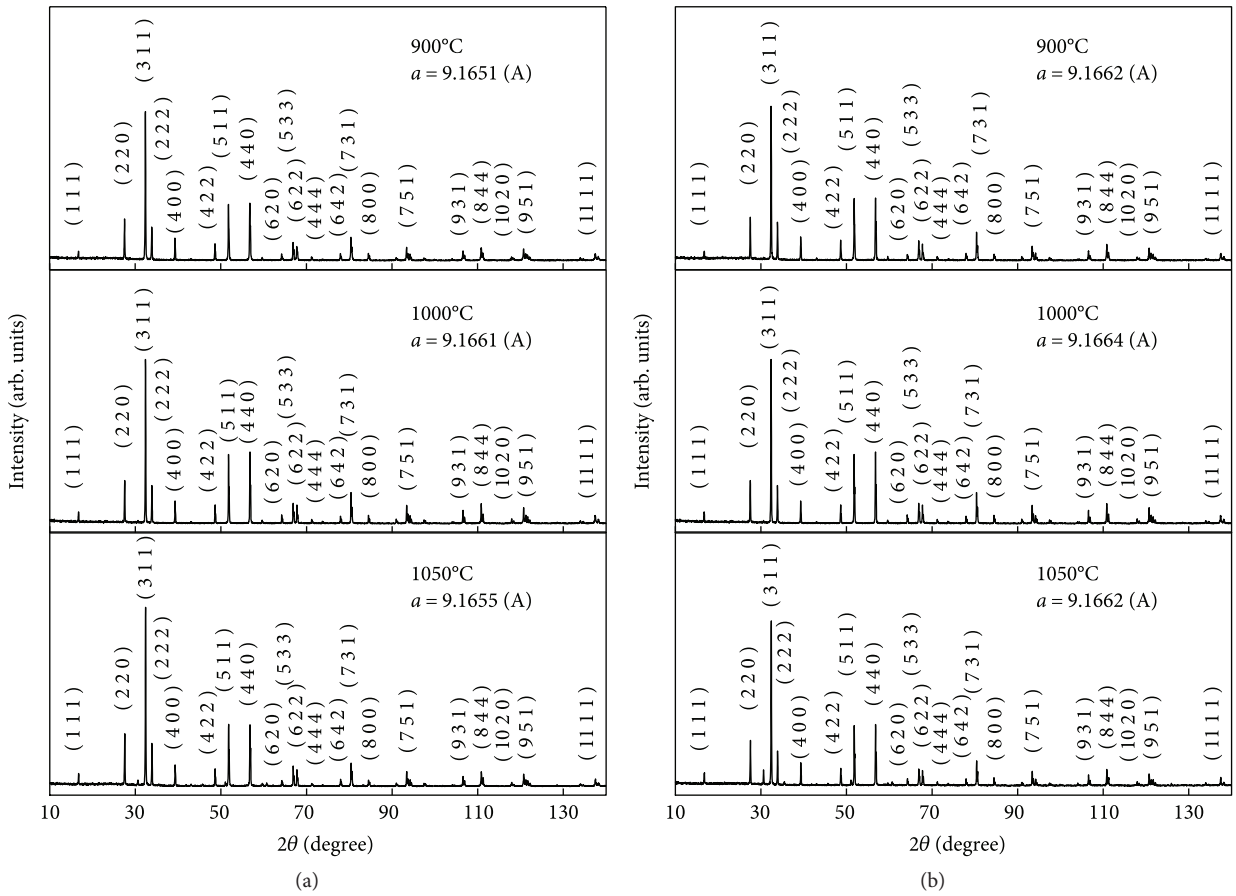

Figure 1: X-ray diffraction patterns of $CdIn_2O_4$ (a) and $CdIn_2O_4$:Er^{3+} (b) crystals.

constant for 24 hours; the crystals were gradually cooled at a descending rate of 10°C/min. The amount of erbium added as an impurity was 1.00 mol%. The structure of the $CdIn_2O_4$ and $CdIn_2O_4$:Er^{3+} crystals was analyzed by X-ray diffractometer (D/MAX-3C, Rigaku Co., Japan). The intensity of the X-ray diffraction pattern peaks was recorded while varying the 2θ angle from 2° to 155° under irradiation with Cu-K_α rays at a wavelength of 1.5405 Å. The X-ray diffraction pattern obtained from the measurement was compared with the interval and peak intensity of the crystal planes provided in the JCPDS card (04-009-5478), and the crystal planes of the measured diffraction pattern were investigated. The lattice constant was calculated using the Nelson-Riley and Riley [9] relationships. The optical absorption properties of the crystals were evaluated in the range of 200~850 nm by using a UV-VIS-NIR spectrophotometer (U-3501, Hitachi, Japan). To determine the optical energy band gap, the optical absorption coefficient (α) corresponding to the energy ($h\nu$) of the irradiation from the absorption spectrum was obtained and the optical energy interval was calculated. The PL characteristics were assessed using a double spectrometer (f = 0.5 m, Acton, Spectrograph 500i, USA) with a PL measurement apparatus comprising a charge coupled device (CCD, PI-MAX3, Princeton Inst. Co., IRY1024, USA). For the PL measurement, the 266 nm line of a diode pumped solid-state (DPSS) laser was used as the excitation source.

3. Results and Discussion

3.1. Crystal Structure. Figure 1 shows the X-ray diffraction patterns of the $CdIn_2O_4$ and $CdIn_2O_4$:Er^{3+} crystals. Figure 1(a) shows the X-ray diffraction patterns of $CdIn_2O_4$ prepared at 900, 1000, and 1050°C. In the case of the pure $CdIn_2O_4$ crystals, distinct diffraction peaks of the (311), (511), and (440) planes were observed. When the temperature was increased from 900 to 1050°C, the peak of the (311) plane became dominant. Figure 1(b) shows the X-ray diffraction patterns of $CdIn_2O_4$:Er^{3+} prepared at 900, 1000, and 1050°C. The diffraction pattern of the $CdIn_2O_4$:Er^{3+} crystals doped with 1.00 mol% of erbium (Figure 1(b)) was the same as that of $CdIn_2O_4$. Figure 1(b) also shows that the main growth plane of the thin film was the (311) plane. Comparison of the experimental X-ray diffraction pattern with the JCPDS card showed that the $CdIn_2O_4$ and $CdIn_2O_4$:Er^{3+} crystals have a cubic crystal structure.

The lattice constants of the $CdIn_2O_4$ crystals were obtained using Nelson-Riley's [9] correction formula, giving respective values of a = 9.1651, 9.1661, and 9.1655 Å for the samples prepared at 900, 1000, and 1050°C, compared with the lattice constant of a = 9.1644 Å from the JCPDS card. When the lattice constant was determined after doping with 1.00 mol% Er^{3+}, a slight decrease was observed according to the temperature used for crystal growth, where values

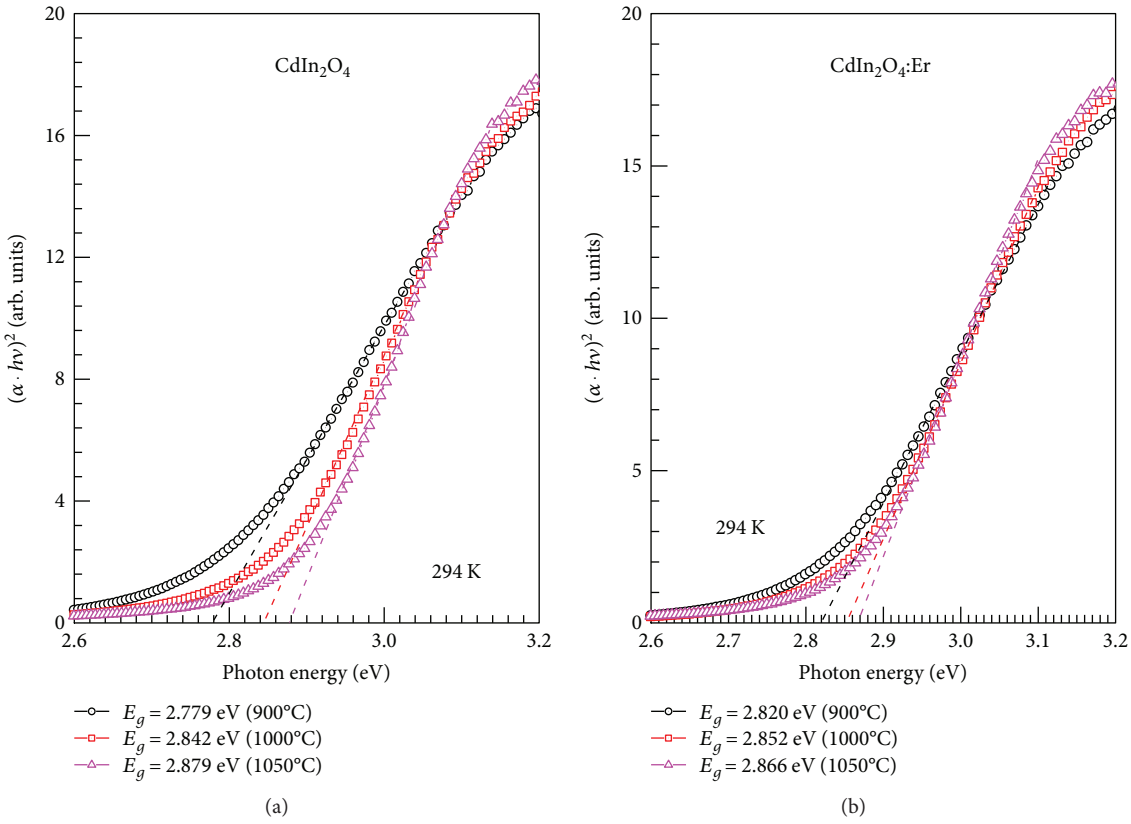

FIGURE 2: Plot of $(\alpha \cdot h\nu)^2$ versus the incident photon energy $(h\nu)$ in $CdIn_2O_4$ (a) and $CdIn_2O_4$:Er^{3+} (b) crystals at 294 K.

of $a = 9.1662$, 9.1664, and 9.1661 Å were obtained for the samples prepared at 900, 1000, and 1050°C, respectively.

3.2. Energy Gaps and Photoluminescence. Figure 2(a) shows the energy gap of the $CdIn_2O_4$ crystals prepared at temperatures of 900, 1000, and 1050°C, where $E_g = 2.779$, 2.842, and 2.879 eV, respectively. Figure 2(b) shows the energy gap of the $CdIn_2O_4$:Er^{3+} crystals prepared at temperatures of 900, 1000, and 1050°C, where $E_g = 2.820$, 2.852, and 2.866 eV, respectively. At the growth temperature of 1050°C, the energy gap of $CdIn_2O_4$:Er^{3+} decreased relatively to that of pure $CdIn_2O_4$, with a shift from 2.879 to 2.866 eV. The energy gap was reduced because Er^{3+}, which replaces indium in the $CdIn_2O_4$ crystal, forms an impurity level between the valence band and the conduction band.

The optical energy gap, Eg, of a semiconductor with a direct band structure can be deduced from the following relation [10]:

$$(\alpha \cdot h\nu)^n \sim (h\nu - E_g), \quad (1)$$

where α is the optical absorption coefficient near the fundamental absorption edge and $h\nu$ is the incident photon energy. The direct energy band gap (E_g) can be obtained when $n = 2$. Figure 2(a) shows the $CdIn_2O_4$ crystal; the direct energy band gap was obtained from Figure 2(a) by extrapolation, giving a value of $E_g = 2.779$~2.879 eV for the $CdIn_2O_4$ crystal at 294 K. Figure 2(b) is plot of $(\alpha \cdot h\nu)^2$ versus $h\nu$ for the $CdIn_2O_4$:Er^{3+} crystals near the fundamental optical absorption edge. The optical energy band gap (E_g) for the $CdIn_2O_4$:Er^{3+} crystals was 2.820~2.866 eV at 294 K, close to 3.0 eV [11].

Figure 3 shows the photoluminescence spectra of the $CdIn_2O_4$ and $CdIn_2O_4$:Er^{3+} crystals, measured at wavelengths of 250~950 nm at 294 K. For the $CdIn_2O_4$ crystals (Figure 3(a)), the photoluminescence peak position changed with increasing crystal growth temperature. For the $CdIn_2O_4$:Er^{3+} crystals (Figure 3(b)), when the crystal growth temperature increased, the position of the emission peak did not change and a narrow and sharp PL peak due to erbium impurities was observed in the 630~700 nm region. These PL peaks are interpreted as arising from electron transfer between the separated electron energy levels of the Er^{3+} ion. Figure 4 shows the photoluminescence spectra of the $CdIn_2O_4$:Er^{3+} crystals grown at 1050°C in the wavelength range of 630~700 nm.

Figure 4 also shows the photoluminescence spectra of the $CdIn_2O_4$:Er^{3+} crystals, measured at wavelengths of 630~700 nm at 294 K. Eight narrow and sharp PL peaks due to erbium impurities were observed in the wavelength region of 651~686 nm. $CdIn_2O_4$ crystallized with a cubic structure in the Fd3m space group. The ionic radius of each component in the $CdIn_2O_4$ crystal is as follows: Cd^{2+}: 0.97 Å, In^{3+}: 0.81 Å, O^{2-}: 0.14 Å. The ionic radius of Er^{3+} is 0.88 Å. When erbium is added to the $CdIn_2O_4$ crystals, the added erbium is most likely to enter the In^{3+}

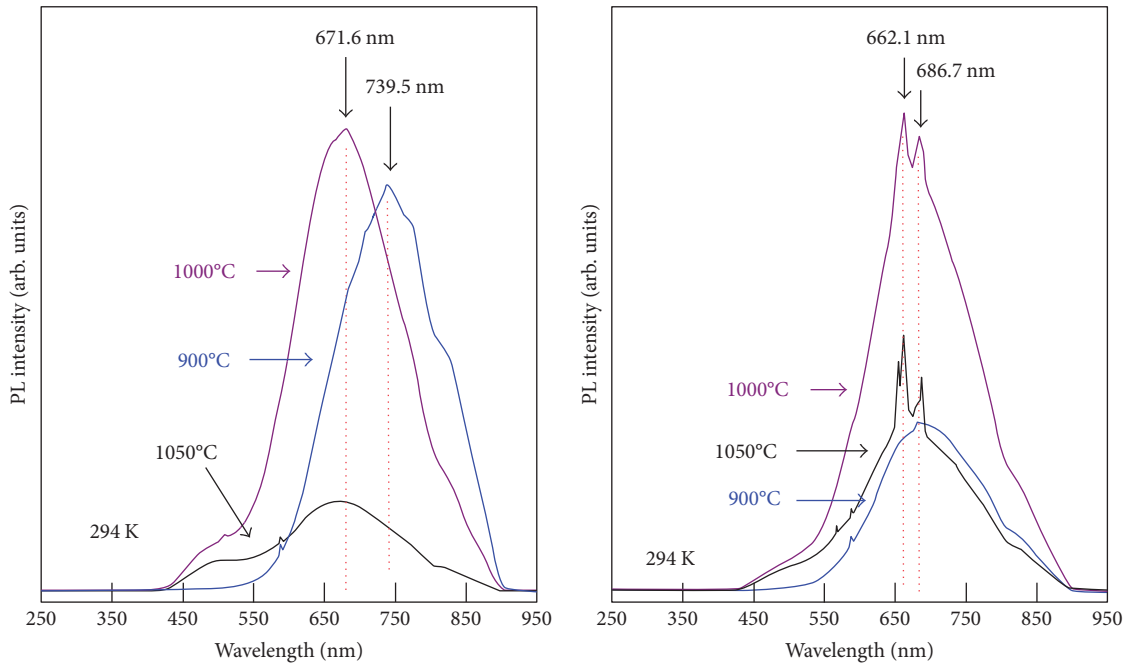

Figure 3: Photoluminescence spectrum of $CdIn_2O_4$ and $CdIn_2O_4:Er^{3+}$ crystals in the range from 250 nm to 950 nm at 294 K.

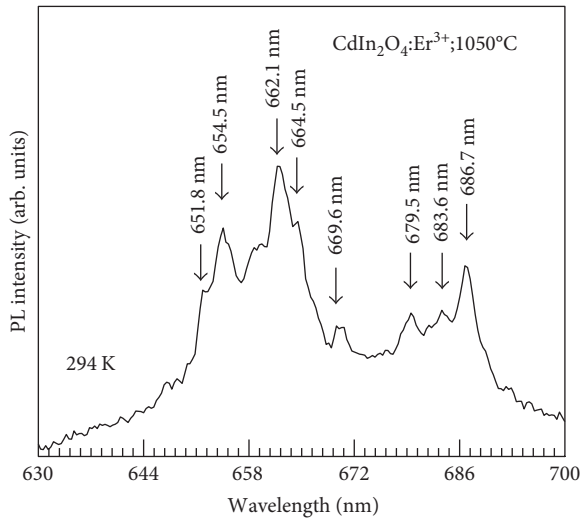

Figure 4: Photoluminescence spectrum of $CdIn_2O_4:Er^{3+}$ crystal in the range from the 630 to 700 nm at 294 K.

sites due to the similar ionic radius; thus, the incorporated erbium in the $CdIn_2O_4:Er^{3+}$ crystal occupies a site of C_{3v} symmetry [12].

4. Conclusion

$CdIn_2O_4$ and $CdIn_2O_4:Er^{3+}$ crystals were grown in a high-temperature electric furnace, and their crystal structures and optical properties were analyzed. The crystal structure of the $CdIn_2O_4$ and $CdIn_2O_4:Er^{3+}$ crystals, determined by X-ray diffraction, was cubic, and the crystals had a direct transition-type energy band structure. At the growth temperature of 1050°C, the energy gap of $CdIn_2O_4:Er^{3+}$ decreased relatively to that of pure $CdIn_2O_4$, with a shift from 2.879 to 2.866 eV. Erbium substituted indium in the $CdIn_2O_4:Er^{3+}$ crystals and narrow and sharp peaks appeared in the region of 651~686 nm due to this effect. These peaks are interpreted as electronic transitions between the energy levels of the Er^{3+} ions located at the site of C_{3v} symmetry.

Conflicts of Interest

The authors declare that there is no conflict of interest regarding the publication of this article.

References

[1] A. Manzar, G. Murtaza, R. Khenata, M. Yousaf, and S. Muhammad, "Electronic and optic properties of cubic spinel CdX_2O_4 (X=in, Ga, al) through modified Becke–Johnson potential," *Chinese Physics Letters*, vol. 31, no. 6, pp. 067401–067404, 2014.

[2] A. Bouhemadou, R. Khenata, D. Rached, F. Zerarga, and M. Maamache, "Structural, electronic and optical properties of spinel oxides: cadmium gallate and cadmium indate," *European Physical Journal Applied Physics*, vol. 38, no. 3, pp. 203–210, 2007.

[3] E. J. J. Martin, M. Yan, M. Lane, J. Ireland, C. R. Kannewurf, and R. P. H. Chang, "Properties of multilayer transparent conducting oxide films," *Thin Solid Films*, vol. 461, no. 2, pp. 309–315, 2004.

[4] X. Wu, T. J. Coutts, and W. P. Mulligan, "Properties of transparent conducting oxides formed from CdO and ZnO alloyed with SnO_2 and In_2O_3," *Journal of Vacuum Science & Technology A: Vacuum, Surfaces, and Films*, vol. 15, no. 3, pp. 1057–1062, 1997.

[5] Z. Szklarski, K. Zakrzewska, and M. Rekas, "Thin oxide-films as gas sensors," *Thin Solid Films*, vol. 174, pp. 269–275, 1989.

[6] F. F. Yang, L. Fang, S. F. Zhang et al., "Structure and electrical properties of $CdIn_2O_4$ thin films prepared by DC reactive magnetron sputtering," *Applied Surface Science*, vol. 254, no. 17, pp. 5481–5486, 2008.

[7] Y. Sun, J. M. Thornton, N. A. Morris, R. Rajpura, S. Henkes, and D. Raftery, "Photoelectrochemical evaluation of undoped and C-doped $CdIn_2O_4$ thin film electrodes," *International Journal of Hydrogen Energy*, vol. 36, no. 4, pp. 2785–2793, 2011.

[8] T. Y. Leswifi, *Synthesis and Photochemical Study of N-doped Mixed Oxide Solid Solution Photocatalyst for Hydrogen Production under Visible Light Irratiation*, Michigan Technological University, ProQuest LLC, Ann Arbor, MI, USA, 2015.

[9] J. B. Nelson and D. P. Riley, "An experimental investigation of extrapolation methods in the derivation of accurate unit-cell dimensions of crystals," *Proceedings of the Physical Society*, vol. 57, no. 3, pp. 160–177, 1945.

[10] J. I. Pankove, *Optical Processes in Semiconductors*, Dover Publications Incorporated, New York, NY, USA, 1971.

[11] D. Ko, K. R. Poeppelmeier, D. R. Kammler et al., "Cation distribution of transparent conductor and spinel oxide solution $Cd_{1+x}In_{2-2x}Sn_xO_4$," *Journal of Solid State Chemistry*, vol. 163, no. 1, pp. 259–266, 2002.

[12] G. H. Dieke, *Spectra and Enerygy Levels of Rare Earth Ions in Crystals*, Wiley, New York, 1968.